Uniform User Interface for Semiautomatic Parking Slot Marking Recognition

Ho Gi Jung, *Member, IEEE*, Yun Hee Lee, *Member, IEEE*, and Jaihie Kim, *Member, IEEE*

***Abstract*—Automatic parking systems consist of three core technologies: 1) target position designation; 2) path planning; and 3) path tracking. Target position-designation methods can be divided into four categories: 1) user-interface based; 2) parking slot marking based; 3) free-space based; and 4) infrastructure based. Considering the fact that parking-assist systems are expected to be used mainly in urban situations, recognition of parking slot markings could be the most economical and efficient solution for target position designation. This paper proposes a semiautomatic parking slot marking-based target position-designation method. The user can initiate parking slot marking recognition by placing a finger on each side of the entrance of the target parking slot. With such a user interface, these systems can reduce the search range to so small an area that computational loads and false-recognition rates are significantly reduced. Furthermore, by identifying the junction patterns of parking slot markings around the designated point with a neural network-based classifier, the user can establish the target position with a uniform user interface. The proposed system showed a 91.10% recognition rate in 191 test cases consisting of five different types of parking slot markings.**

***Index Terms*—Distance transform (DT)-based localization, driver-assistant system, parking-assist system, semiautomatic parking slot marking recognition.**

I. Introduction

AUTOMATIC parking systems consist of three components: 1) target position designation; 2) path planning; and 3) path tracking by active steering. The methods of target position designation can be divided into four categories: 1) user-interface based; 2) parking slot marking based; 3) free-space based; and 4) infrastructure based. A detailed survey can be referred to in [1]. Considering the fact that parking-assist systems are expected to be used mainly in urban situations, recognition of parking slot markings could be the most economical and efficient solution for target position designation. If parking slot marking recognition is done without the help of a driver, it is called automatic [2]–[5]. Conversely, semiautomatic approaches utilize the user's input assumption that the user is willing to provide useful information to reduce the search range and improve the recognition performance [7]–[9].

Automatic recognition systems use various kinds of constraints to enhance the efficiency of parking slot marking recognition. Assuming that the parking slot markings are drawn with a specific color, Xu *et al.* extracted pixels belonging to the parking slot markings by applying restricted Coulomb energy neural-network-based color segmentation [2]. The system shown in [3] separated pixels on the ground surface by reconstructing 3-D information with a binocular stereo camera and checking whether each pixel meets the ground surface homography. In [4], one constraint of a parking slot marking's drawing was used; parking slot markings consist of line segments with a fixed width. The system made a bird's-eye view edge image from an input image captured with a fisheye lens and then transformed into Hough space. As two edges of a parking slot marking line segment form a pair of parallel lines with a fixed distance, they could be detected by finding a specific pattern in the Hough space. The system detected parking slot marking line segments using specifically designed 1-D filtering in the Hough space. Tanaka *et al.* proposed a system constantly calculating the virtual target position based on the vehicle position and deflection angle just before backing up [5]. By using the virtual target position as the region of interest (ROI), the system not only enhanced the recognition performance but reduced the processing time as well. Then, the system eliminated the outliers and detected straight lines using an improved random sample consensus algorithm, which had a high degree of robustness and was superior in calculation cost than the Hough transformation.

In spite of the development of automatic parking slot marking recognition and free-space-based systems, a user-interface-based system is still required because it is an economical solution and can provide an essential backup tool when automatic methods fail [6]. If there is a user interface supporting an easy-to-use input method such as a touchscreen, then users are expected to willingly provide useful information for target position designation. Our previous work [7] showed that if a driver designated the target position by touching a point inside a rectangular parking slot marking on a touchscreen-based human–machine interface (HMI), then the target position could be designated with confidence, and the required computation could be minimized. Although the method drastically reduced the search range, it had one serious drawback in that it could only be applied to a rectangular parking slot marking type.

To generalize semiautomatic parking slot marking recognition and establish a uniform user interface, this paper proposes a novel target position-designation method where the driver

Manuscript received April 10, 2009; revised August 25, 2009 and October 1, 2009. First published October 20, 2009; current version published February 19, 2010. This work was supported by the Korea Science and Engineering Foundation under Grant R112002105070010(2009) through the Biometrics Engineering Research Center, Yonsei University. The review of this paper was coordinated by Dr. Y. Gao.

H. G. Jung and J. Kim are with the Biometrics Engineering Research Center, Yonsei University, Seoul 120-749, Korea (e-mail: hgjung@yonsei.ac.kr; jhkim@yonsei.ac.kr).

Y. H. Lee is with the Global R&D H.Q., MANDO Corporation, Yongin 446-901, Korea (e-mail: p13446@mando.com).

Color versions of one or more of the figures in this paper are available online at http://ieeexplore.ieee.org.

Digital Object Identifier 10.1109/TVT.2009.2034860

Fig. 1. Driver designates target position by pointing out two ends of the target parking position's entrance.

points out the target by placing a finger on each side of the entrance of the target parking slot, as shown in Fig. 1. As the driver cannot be expected to exactly designate the entrance position, the proposed system searches for the exact position by recognizing parking slot markings. This approach has three advantages over the previous methods. 1) Unlike [7], it does not need to assume that the parking slots and roadways are separated by a line. Therefore, it can be applied to various kinds of parking slot marking types. 2) As what to recognize is directly pointed out, the ROI can accurately be established. Therefore, the computational load and memory requirement for fisheye lens-related rectification and bird's-eye view image construction can significantly be reduced. 3) It does not require additional camera and operating skills as in [8]. Although the basic idea of this interface was originally proposed in [9], this paper completes the proposed method by automating the parking slot marking-type selection with neural-network-based-type recognition and using one localization algorithm instead of a type-dependent algorithm.

Fig. 2 shows the flowchart for the proposed method. By setting the gear position to "R," the driver can initiate the parking-assist system. The system captures a rearview image with a rearward camera installed at the back end of the vehicle and then displays the image through HMI. The driver designates the target position by pointing out two seed points with the touchscreen-based HMI. After applying fisheye lens-related rectification and bird's-eye view image construction to the region around each seed point, the type of junction pattern is recognized by the neural-network-based classifier. The junction pattern denotes a particular pattern of parking slot marking that is supposed to exist around the seed point. With a template corresponding to the recognized class, the junction pattern is searched by template matching with the skeleton of parking slot markings. If there is definitely a junction pattern present, then the junction pattern searching is equal to finding the placement of a junction pattern that minimizes the matching error. Once two junction patterns are detected, the coordinates of the entrance of the target slot are fixed. Therefore, the coordinates of the target position can be established. Consequently, based on the coordinates of the target position, a path can be planned.

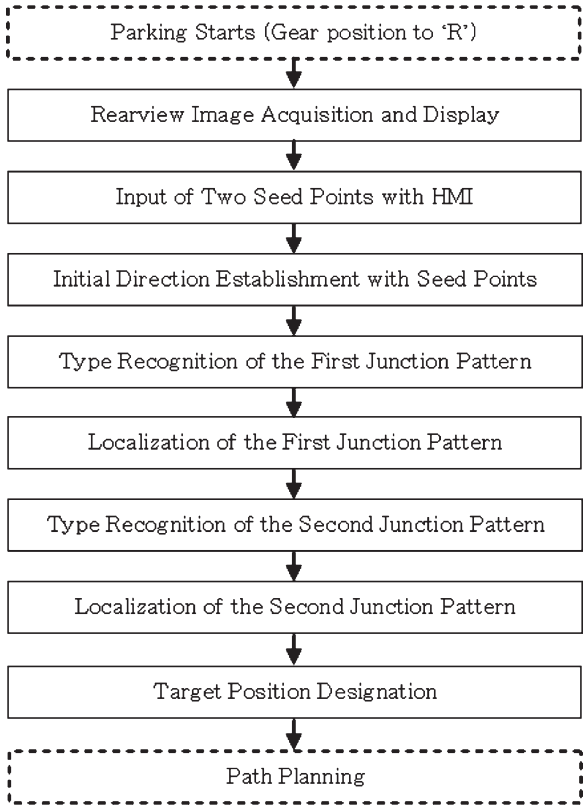

Fig. 2. Flowchart of the proposed method.

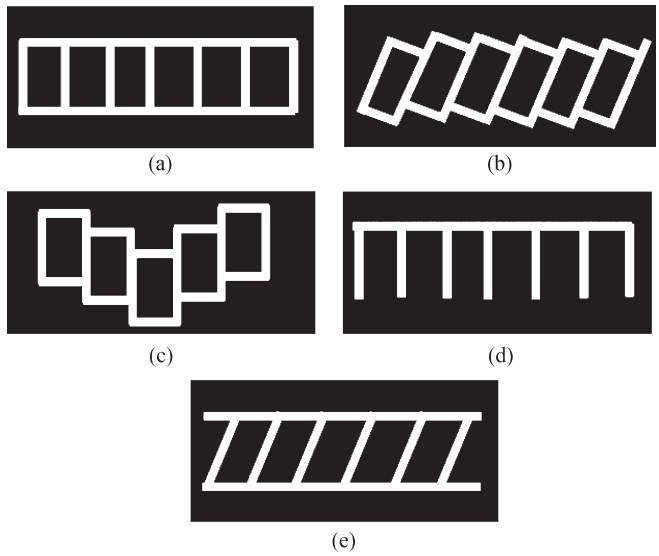

Fig. 3. Five types of parking slot markings. (a) Rectangular type. (b) Slanted rectangular type. (c) Uneven rectangular type. (d) Open rectangular type. (e) Diamond type.

II. Parking Slot Marking Types and Junction Pattern Types

Although there are various types of parking slot markings, the five types depicted in Fig. 3 are the most commonly used: 1) rectangular; 2) slanted rectangular; 3) uneven rectangular; 4) open rectangular; and 5) diamond type. When the driver places a finger on each side of the entrance of the target parking slot according to the proposed method, the parking

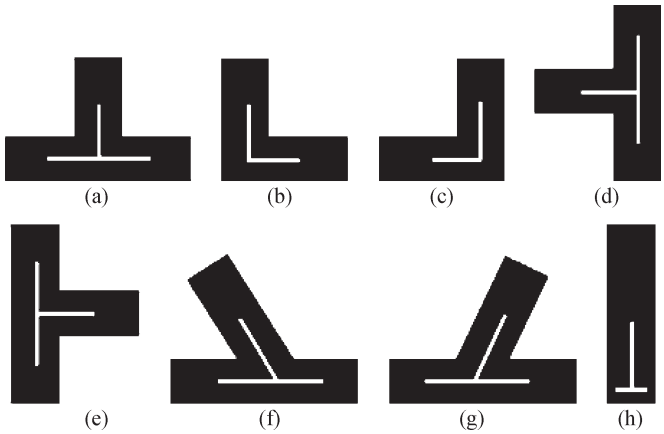

Fig. 4. Junction pattern classes and corresponding templates. (a) Class 1. (b) Class 2. (c) Class 3. (d) Class 4. (e) Class 5. (f) Class 6. (g) Class 7. (h) Class 8.

slot markings closest to the area indicated, which are called the junction pattern, are important for the exact localization of the target parking slot. It is found that the junction patterns of those five parking slot marking types can be categorized into eight classes, as depicted in Fig. 4; each of them is classified from 1 to 8, respectively. The black rectangles represent the junction pattern, in which two white line segments are drawn to show the template of the corresponding class. A template consisting of two line segments is used for junction pattern localization. The crosspoint of the line segments is called the center point, which denotes the location of the junction pattern. The direction of the upward line segment denotes the junction pattern direction in six cases. In the cases of classes 4 and 5, the direction of the line segment pointing laterally denotes the junction pattern direction.

III. Region of Interest Setting and Junction Pattern Class Recognition

In the proposed method, the driver is expected to point out both sides of the entrance of the target parking slot, although they may not be completely accurate. As recognized junction patterns can establish the target position, our problem could be simplified as having to search for two junction patterns close to the respective seed point. The ROI bird's-eye view image construction and junction pattern class recognition will be explained.

A. Three Coordinate Systems

The rearward camera uses a fisheye lens to maximize the view behind the vehicle. The relation between the input image coordinate system and the rectified image coordinate system, i.e., the undistorted image coordinate system, can be expressed by a fifth-degree polynomial of distance with respect to the image center [10]. Therefore, these two coordinate systems have a one-to-one relation. As the rearward camera is installed at a fixed height and with a fixed angle, the relation between the rectified image coordinate system and the bird's-eye view image coordinate system can be expressed by homography

Fig. 5. One-to-one relation between three coordinate systems.

H [11]. If a point is (x, y) in the camera coordinate system, then the coordinates of the corresponding point on the ground (v_x, v_y) can be calculated by

$$v_x = \frac{H_C x \cos\theta + (y \sin\varphi - f \cos\varphi) H_C \sin\theta}{y \cos\varphi + f \sin\varphi}$$
$$v_y = \frac{H_C x \sin\theta - (y \sin\varphi - f \cos\varphi) H_C \cos\theta}{y \cos\varphi + f \sin\varphi} \quad (1)$$

where H_C, φ, and θ denote the height from the ground, the pitch angle, and the yaw angle of the camera, respectively. f is the focal length. Therefore, these two image coordinate systems have a one-to-one relation as well. Consequently, a point in the input image and a point in the bird's-eye view image have a one-to-one relation, as shown in Fig. 5.

B. ROI Establishment by Two Seed Points and Bird's-Eye View Image Construction

It can be assumed that a region with a fixed area close to a seed point contains only one junction pattern because the point input by the driver is expected to be close to the endpoint of the left or right side of the parking slot. How wide an area should be searched is influenced by touch screen size, the driver's operational characteristics, and the tradeoff between success rate and system resource. In this paper, a 1 m $\times$ 1 m area around a seed point is used as the ROI. As the orthogonal direction to a line connecting two seed points and outward from the camera is expected to be similar to the direction of the junction pattern, the vertical direction of the ROI is set to it. The ROI bird's-eye view image is constructed by copying intensity values of corresponding pixels in the input image. As only a small region around the seed point is transformed into a bird's-eye view image and no interpolation is used, memory consumption and computational load are restricted within a small amount. Fig. 6 shows an example of a constructed ROI bird's-eye view image. Two seed points inputted by the driver in the case of an uneven rectangular type are depicted by two small circles, and the "T" shape represents the initial direction of the parking slot. Two images in a rectangle close to the seed point show the constructed ROI bird's-eye view image corresponding to the seed point, respectively. The left junction pattern is class 2, and the right is class 4 (the class index is defined in Fig. 4).

C. Neural-Network-Based Junction Pattern Class Recognition

As the ROI bird's-eye view image is constructed based on seed points inputted by the driver, the center point location and the direction of the junction pattern are supposed to contain

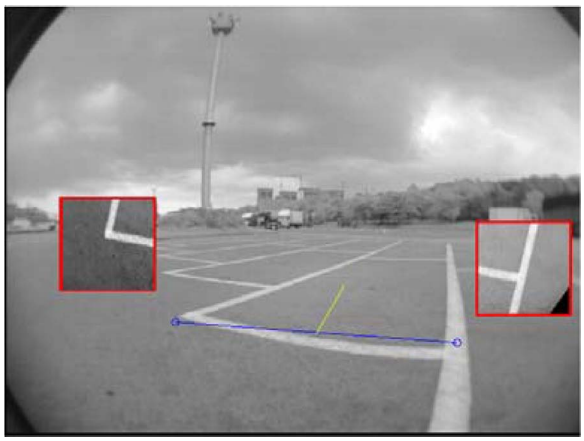

Fig. 6. Construction of ROI bird's-eye view image corresponding to two seed points.

more or less noise. However, as the junction pattern is drawn with a light color on a dark ground surface and has a limited range of shapes, it can be classified with a three-layered neural network. The ROI bird's-eye view image, which originally was a 2-D matrix, is converted into a 1-D array by lexicographical order and then fed into the input layer. The output layer has nodes corresponding to eight junction pattern classes. The neural network is trained such that only one node corresponding to the input image's class becomes 1, and the others are 0. The learning method and the node number of the hidden layer will be explained in Section V.

IV. Junction Pattern Localization and Target Position Establishment

If it is assumed that there is only one junction pattern in an ROI bird's-eye view image, then junction pattern detection is equal to a problem searching the optimal coordinates and orientation of the junction pattern. Once the locations of two junction patterns are exactly recognized, the target position can easily be established by taking into account the recognized junction pattern classes.

A. Binarization

In general, as parking slot markings are drawn with a light color on a darker ground surface, the rectified image can be segmented into two regions: 1) parking slot marking and 2) ground surface. However, because of shadows beneath vehicles and asphalt texture patterns, it is hard to extract regions corresponding to parking slot markings from an actual outdoor image. As a solution, clustering in an intensity histogram is applied: the intensity histogram is overclustered into clusters, and the brightest cluster is regarded as the pixel belonging to the parking slot markings. Although overclustering causes a noisy contour for parking slot markings, it can extract the pixels from the parking slot markings with less cost compared with time-consuming segmentation methods [12]. To eliminate small blobs and noisy contours, a binary image is processed twice by a binary morphological operation "majority." The "majority" operation sets a pixel to 1 if five or more pixels in its three-by-three neighborhood are 1's. Otherwise, it sets the pixel to 0 [13]. Fig. 7 shows the binarization procedure: (a) shows one of the ROI bird's-eye view images of Fig. 6. Fig. 7(b) and (c) shows the resultant image of clustering in an intensity histogram and the extracted pixels, respectively. Finally, Fig. 7(d) shows the result of "majority" operation.

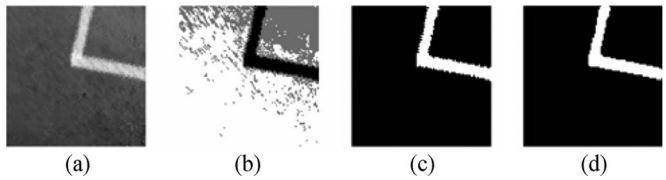

Fig. 7. Binarization procedure. (a) Original Image. (b) Clustered Image. (c) Pixels of the brightest cluster. (d) Resultant image.

B. Localization by Template Matching With Skeleton

As the proposed method does not assume the width of the line segments constructing a junction pattern, the junction pattern is localized by searching the optimal transformation that maximizes the overlap between the skeleton of the binary image and the class template. The transformation is denoted by (x, y, θ), where (x, y) denotes the center point coordinates of the junction pattern template, and θ denotes the orientation of the junction pattern template. To measure how well they are quantitatively overlapped, the distance transform (DT) of the skeleton is used. The error of a transformation is defined as the mean DT value over the line segments constructing the class template, which is transformed by the transformation and overlapped on the DT of the skeleton. The transformation error defined in this way will be 0 when the template is exactly overlapped on the skeleton and increases as the template mismatches the skeleton. Furthermore, it is proven that even a disconnected and noisy skeleton can be used for junction pattern localization by minimizing the error [14].

Therefore, the junction pattern localization problem is converted into an error-minimization problem. The proposed method solves this problem by genetic algorithm (GA). An individual consists of three genes corresponding to the placement parameters of the junction pattern template, and the fitness function is defined as the error of the placement with respect to the skeleton's DT. To enhance the efficiency of the GA, θ is restricted to a range similar to the initial longitudinal direction of the target position, and the center point coordinates of the target pattern template are initialized with the intersection and endpoint of the skeleton. As the endpoints are useful in the case of a disconnected skeleton, they are ignored when they are close to an intersection. The intersections and the endpoint of the skeleton are detected by a simple method that investigates eight neighbors of a pixel [15], [16].

Fig. 8 shows the junction pattern localization procedure of the binary image in Fig. 7(d), where the junction pattern is class 2: Fig. 8(a) is the skeleton of Fig. 7(d), and Fig. 8(b) shows the initial set of the template center point using intersections and endpoints. Fig. 8(c) shows the DT of a given skeleton, where the smaller value is darker, and the larger value is brighter. Finally, Fig. 8(d) draws a junction pattern over the

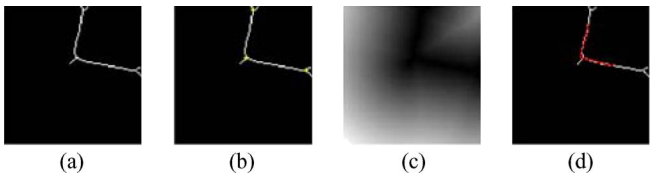

Fig. 8. Localization procedure. (a) Skeleton. (b) Initial center points. (c) DT of skeleton. (d) Detected position.

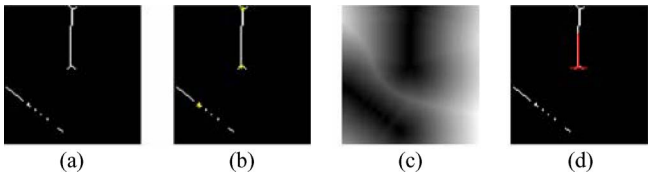

Fig. 9. Localization procedure when junction pattern is class 8. (a) Skeleton. (b) Initial center points. (c) DT of skeleton. (d) Detected position.

skeleton after applying the optimal transformation found as the optimization result. Fig. 9 shows the localization result when the junction pattern is class 8. As the proposed localization method finds a transformation that best suits the shape of the junction pattern template, it can detect parking slot markings, even with additional skeletons from noise, as shown in Fig. 9(a). It is noticeable that the proposed localization method uses a common procedure, even with an open rectangular type by utilizing the fact that the skeleton of junction pattern class 8 forms a small "T" shape. It is different and improved from our previous implementation [9].

C. Target Position Establishment

Once the junction patterns on both sides of the entrance of the target parking slot are recognized, the target position can accordingly be established. For four types excluding the diamond type, the target position can be established by placing the lateral side of the rectangular target position on a line connecting the center points of two junction patterns and locating the lateral center of the rectangle on the middle point of two junction patterns, as shown in Fig. 10(a). The width and length of the rectangle is the same as those of the subject vehicle. In the case of the diamond type, the rectangle of the target position does not meet the line connecting two junction pattern center points. Instead, a point to which one of the two junction pattern center points is projected is used: If the junction pattern is class 6, then the left is used, and if it is class 7, then the right is used. The line connecting a junction pattern and its projection is orthogonal to the direction of two junction patterns, as shown in Fig. 10(b).

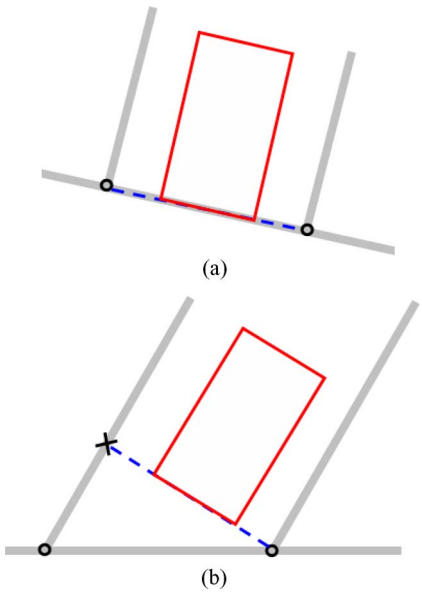

Fig. 10. Target position establishment. (a) Four types except diamond type. (b) Diamond type.

V. Experimental Results

A. Optimal Parameter of Neural Network

The neural network for the junction pattern classifier was implemented using the MATLAB Neural Network Toolbox [17], and the learning algorithm used was the scaled conjugate gradient (SCG) method [18]. The basic backpropagation algorithm adjusts the weights in the steepest descent direction (negative of the gradient): the direction in which the performance function is decreasing most rapidly. It turns out that, although the function decreases most rapidly along the negative of the gradient, this does not necessarily produce the fastest convergence. In the conjugate gradient algorithms, a search is performed along conjugate directions, which produces a generally faster convergence than the steepest descent directions. SCG is a variation of conjugate gradient that was designed to avoid a time-consuming line search. SCG is selected because it is expected to require fewer computation numbers for each iteration and fewer storage requirements [17].

The neural network consists of three layers. The input layer is designed to get the ROI bird's-eye view image (size 101×101) directly in the form of a 1-D vector, and the output layer is designed to have eight nodes corresponding to each junction class. The hidden layer node and the output layer node use the logarithmic sigmoid function as the output function. The neural network learning process used a learning data set (1534 images) and was repeated until the mean square error (MSE) became below $1e-5$ or the iteration number exceeded 10 000. The percentage of each class from 1 to 8 in the learning data set is 13.32%, 6.24%, 25.15%, 11.76%, 7.08%, 14.04%, 14.75%, and 7.67%, respectively.

Performance with respect to the hidden layer node number was evaluated to determine the hidden layer node number, which was one of the parameters that significantly influenced the performance of the neural network-based classifier. While increasing the node number from 10 to 140 by 10, the neural network was trained ten times, and the median MSE was measured [see Fig. 11(a)]. As the MSE is almost 0, and the recognition rate is 100% when the node number is greater than 50, the hidden layer node number was set to 60.

Performance with respect to the learning sample size was evaluated to give a rough guideline to how many samples are required for sufficient performance. While increasing the learning sample size from 10% to 100% by 10% of the total learning data set (1534 images), the neural network was trained ten times, and

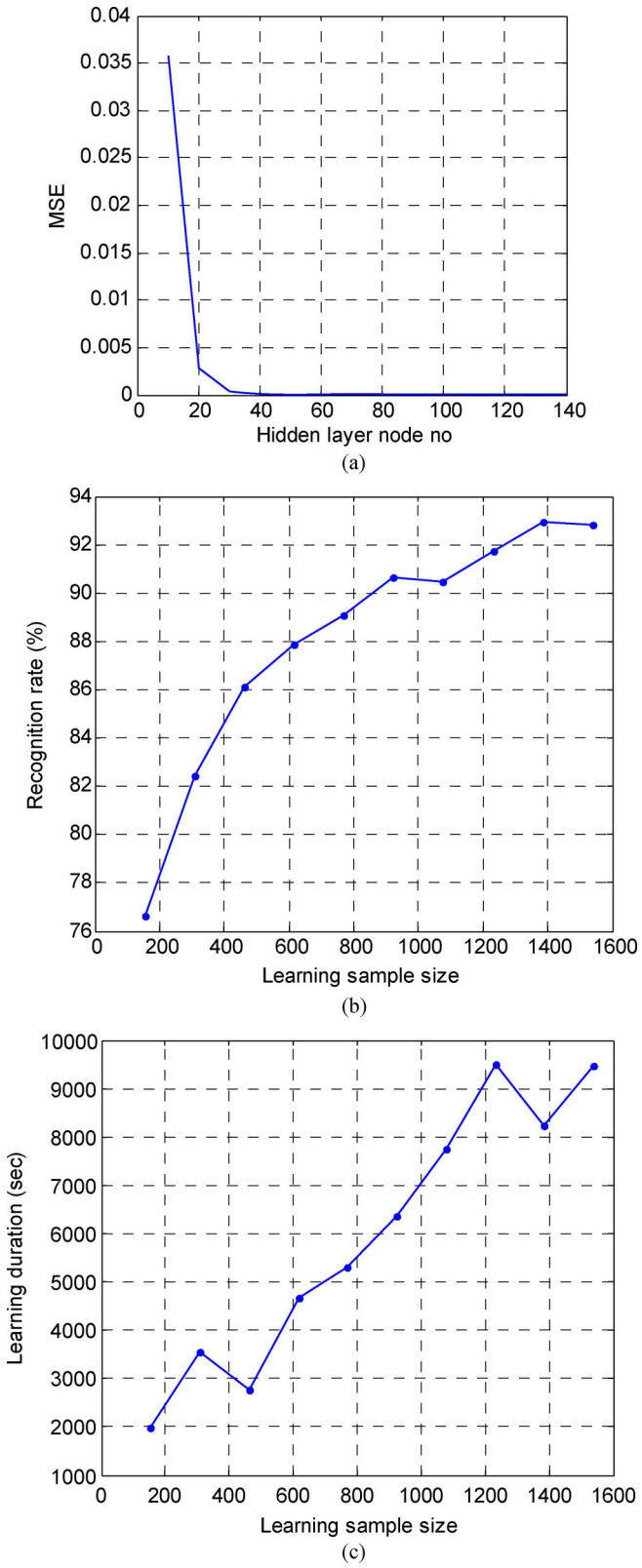

Fig. 11. Learning results of junction pattern classifier. (a) Junction pattern classifier performance with respect to hidden layer node number. (b) Junction pattern classifier performance with respect to learning sample size. (c) Junction pattern classifier learning duration with respect to learning sample size.

the average recognition rate and the average learning duration were measured [see Fig. 11(b) and (c), respectively]. For every learning, the learning sample set was randomly selected from the total learning data set. The recognition rate was measured with 382 samples, which are not used for learning. At around 1400 samples, the recognition rate seems to be saturated, as shown in Fig. 11(b). Considering that the time needed for learning is proportional to the learning sample size, as shown in Fig. 11(c), the sample size used (i.e., 1534) looks reasonable.

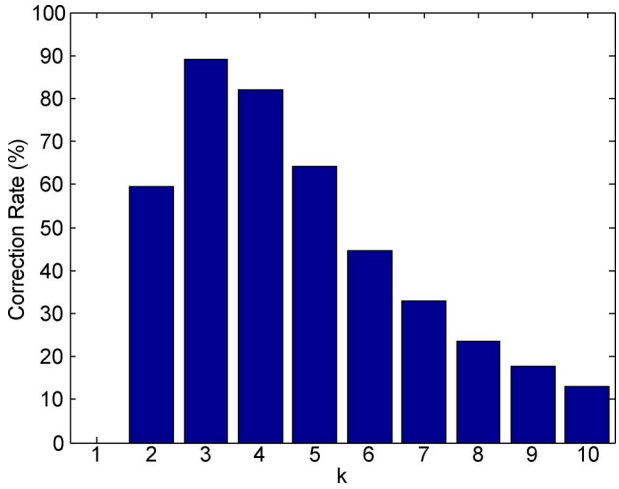

Fig. 12. Binarization correction rate with respect to the cluster number of k-nearest neighbor clustering in intensity histogram.

B. Optimal Parameter of Binarization

Binarization performance with respect to the cluster number was evaluated to determine the cluster number, which is the most important parameter of intensity histogram clustering-based binarization. While changing the cluster number k from 2 to 10 when applying k-nearest neighbor clustering to the intensity histogram, whether the cluster with the largest mean value could extract parking slot markings well or not was manually evaluated. The evaluation was conducted with the learning data set, and the result is shown in Fig. 12. Cases determined as a failure include when the resultant parking slot marking contains too much noise, when the marking is severely erased, and when other objects, e.g., asphalt surface, is extracted as a marking. Consequently, when $k = 3$, the evaluation result shows the best correction rate (i.e., 89.1%).

Fig. 13 shows various binarization results. Fig. 13(d) shows that intensity histogram-based clustering with $k = 3$ can successfully extract parking slot markings, even when an adjacent vehicle is partially shown and illumination is different locally. Fig. 13(e) shows when binarization with any k value cannot extract parking slot markings because an image is reflected on a wet ground surface and the modals of the intensity histogram are not sufficiently sharp. The extraction of parking slot markings fails most frequently due to the presence of reflected images from nearby obstacles or strong reflected sunlight when the ground surface is wet. Therefore, these cases can be regarded as the major reasons for binarization failure.

C. Optimal Parameters of GA-Based Localization

Junction pattern localization by GA-based optimization was implemented using the MATLAB Genetic Algorithm

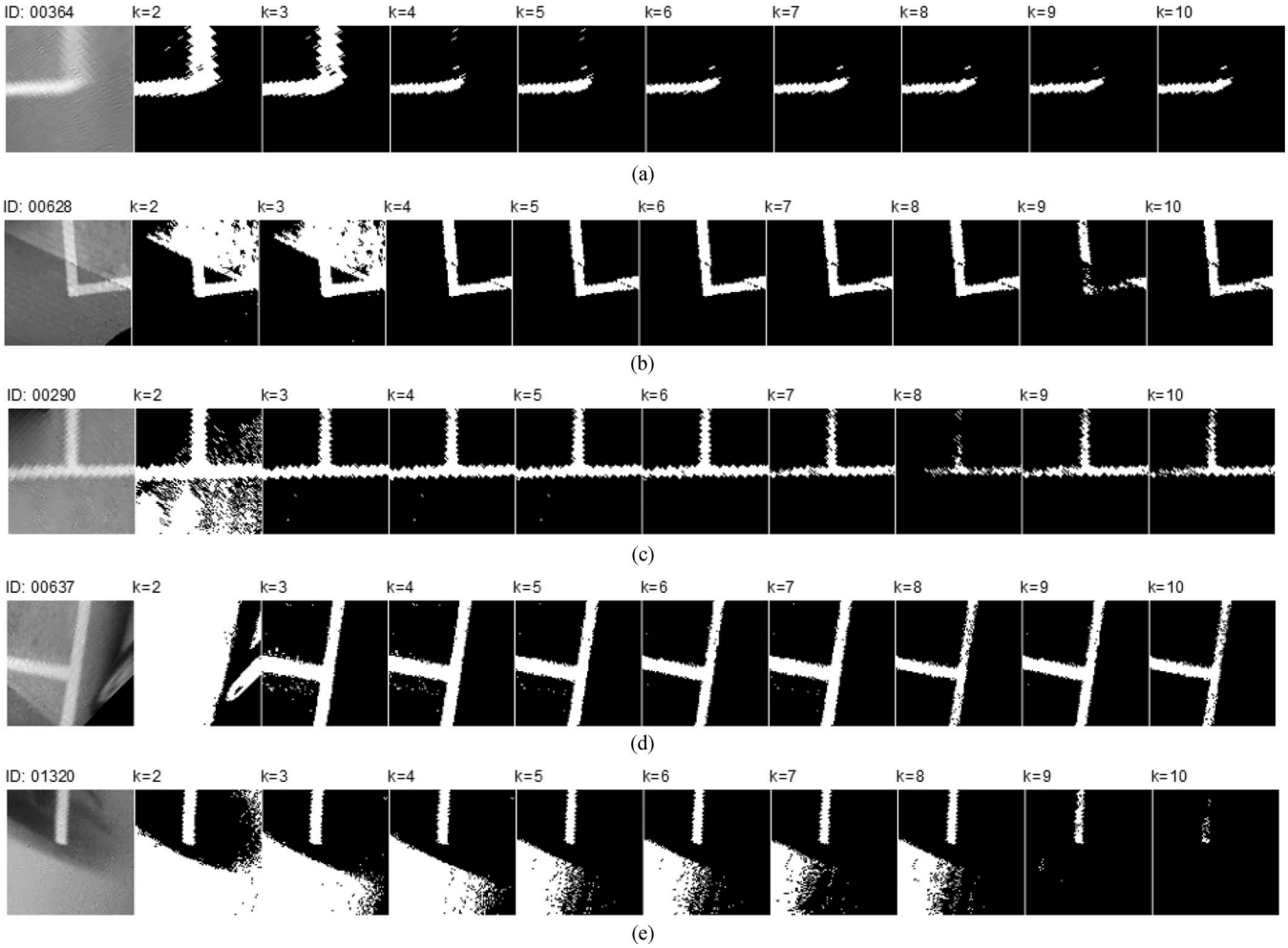

Fig. 13. Binarization results. (a) Typical example: successful when $k = 2, 3$. (b) Successful when $k = 4{-}8$ and 10. This is the case when more than two clusters are generated because of locally different colors of the ground surface. (c) Successful when $k = 3{-}7$. This is the case when more than two clusters are generated because of illumination variation. (d) Successful when $k = 3{-}10$. Binarization succeeds in spite of ground surface texture and obstacles. (e) All k values fail because of wet ground surface.

Toolbox [19]. To determine the most important parameters (population size and generation number), localization performance was evaluated while changing these two parameter values. One hundred samples were randomly selected from the learning data set, and then, the ground truth of junction pattern location and orientation was established by applying GA-based junction pattern localization with a sufficiently large population size and generation number (200 and 100, respectively) and manually verifying the validity. While changing the population size from 10 to 200 by 10 and the generation number from 10 to 100 by 10, respectively, the MSE of the junction pattern center coordinates and orientation with respect to the ground truth was measured (see Fig. 14). It can be observed that localization performance becomes saturated when the population size is greater than 100 and the generation number is greater than 50.

To validate the established parameter values, localization performance was measured with the learning data set; the success rate was 98.18%. Because the neural network-based junction pattern classifier showed a 100% recognition rate regarding the learning data set, the class of each image could correctly be recognized. An important point is that although the success rate of binarization was 89.1%, the success rate of

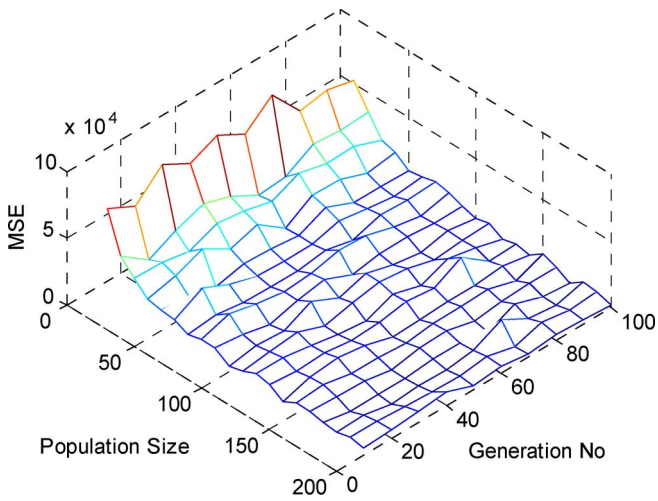

Fig. 14. Junction pattern localization performance with respect to GA-related parameters.

localization reached up to 98.1%. This phenomenon is thought to be caused by the fact that the correct junction pattern class enables localization to find optimal position and orientation

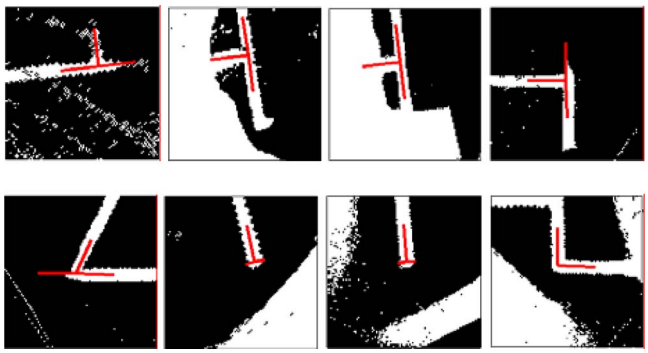

Fig. 15. Cases when localization succeeds in spite of binarization failure.

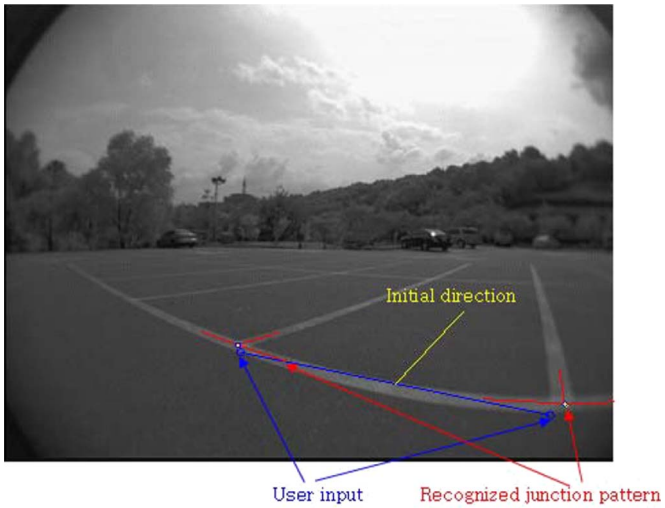

Fig. 16. Driver's inputs and recognized junction patterns.

by using the correct template in spite of binarization failure. Fig. 15 shows the examples.

D. Recognition Performance

Recognition performance was evaluated by applying the proposed method to 191 cases. The number of the parking slot type is 65, 40, 14, 45, and 27, respectively. The recognition rate corresponding to each type is 92.30%, 90.00%, 92.86%, 86.67%, and 96.30%, respectively. Fig. 16 shows an example of a seed point inputted by the driver and the recognized junction pattern. The resolution of the input image is 640 × 480. Fig. 17 shows the junction pattern-recognition result and the established target position for each type. The reason why the recognition rate of the diamond type is somewhat lower than the others' is due to the fact that an incorrect junction pattern class causes the establishment of an incorrect target position.

The junction pattern of all parking slot marking types, except the diamond type, plays the same role in the establishment of the target position. As the junction pattern center points designate both side endpoints of the parking slot entrance, and the orthogonal direction to a line connecting these two points is the direction of the parking slot, even when a junction pattern is incorrectly recognized, it can successfully establish the target position. In Fig. 18(a), although the right junction pattern of class 1 is incorrectly recognized as class 3, the target position

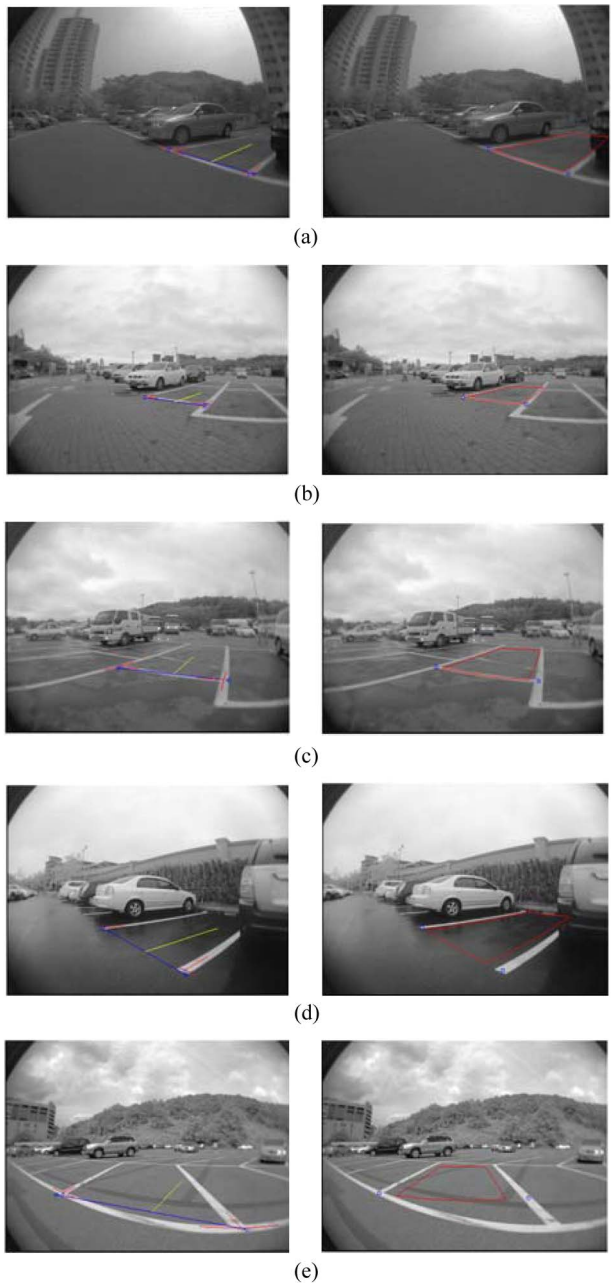

Fig. 17. Parking slot marking recognition result. In the left column, the driver's inputs are depicted by small circles, and the initial direction of the target position is depicted by a large "T." The result of junction pattern recognition is expressed by drawing a template corresponding to the class. In the right column, the finally established target position is depicted by a rectangle, and the center point of the recognized junction pattern is depicted by a small circle. (a) Rectangular type. (b) Slanted rectangular type. (c) Uneven rectangular type. (d) Open rectangular type. (e) Diamond type.

is correctly established. In Fig. 18(b), the right junction pattern of class 3 is incorrectly recognized as class 8, but the target position is correct.

There are two major causes of recognition failure. The first is when there are more than three modals in the intensity histogram of the ROI bird's-eye view image: when there is too much image reflected on a wet ground surface, when reflected sun light is too strong [as shown in Fig. 19(a)], when the texture of the ground surface is too complicated, and when illumination is different locally. The second is when the junction pattern

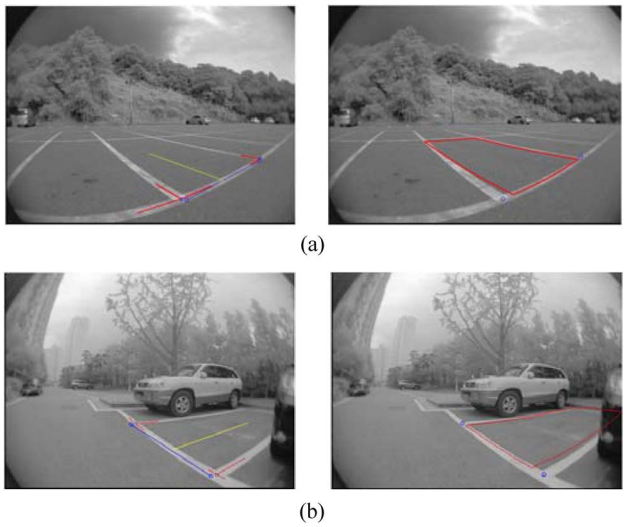

Fig. 18. Cases when the target position is correctly established in spite of an incorrect junction pattern classification. (a) The right junction pattern is class 1 but incorrectly recognized as class 3. (b) The right junction pattern is class 3 but incorrectly recognized as class 8.

Fig. 19. Causes of failure of target position establishment. (a) Wet ground surface. (b) Wrongly recognized junction pattern class.

class is incorrectly recognized. In particular, if the parking slot is of the diamond type, an incorrectly recognized junction pattern causes a false target position, as shown in Fig. 19(b).

E. Discussion

The proposed method requires much less computation and memory compared with [3] acquiring the vertical edge of stereo images and finding their correspondences and [4] applying fisheye lens rectification and bird's-eye view transformation to the whole input image. In our previous work [3], we tried to reduce the computational load by only considering vertical edge pixels, which reached 7.8% of input image pixels: $7.8\% \times 640 \times 480 = 23\,962$. Although it is almost the same as the ROI area of the proposed method $(2 \times 101 \times 101 = 20\,402)$, each pixel was investigated to find the correspondence by applying 3×3 mask-based correlation and 5×5 mask-based color correlation in the ± 35 disparity range. Furthermore, the system in [3] involved the construction of an obstacle depth map and a bird's-eye view image of the same specification as [4]. If the proposed method is compared with our other previous work [4], then the most important factor might be the amount of lens distortion rectification and bird's-eye view transformation. Considering that the amount is proportional to the result image area, the proposed method only requires 5.83% of [4]: The result image size is 2 (because of two junction patterns) $\times$ 101 $\times$ 101 in the proposed method and 500 $\times$ 700 in [4], respectively. Although the neural network of the proposed method requires a significant amount of computation, it is nothing compared with the heavy Hough transform and edge following in [4].

Fig. 20. Effect of polarizing filter: eliminating strong sunlight reflected on wet ground surface. (a) Captured without a polarizing filter. (b) Captured with a polarizing filter.

Furthermore, the proposed method is expected to shorten the operation time and enhance the driver's acceptability as it requires fewer clicks, i.e., just two clicks, whereas [6] requires an average of six to nine clicks. By resolving the drawbacks of [7] requiring a line separating the parking area and roadway and the inconvenience of [8] requiring the driver to designate the type of parking slot markings, the proposed method completes the semiautomatic parking slot marking recognition that minimizes the search area based on the driver's input and utilizes the junction pattern class for its localization. In particular, it enables the driver to use a parking-assist system with uniform user interface for various kinds of parking slot types and is expected to enhance the driver's intuitive understanding of the system.

Although [8] was developed to recognize three types of parking slot markings, it requires an additional camera installed on the subject vehicle's side surface and directed laterally. Such an installation is quite different from usual cases and seems difficult to manage in relation to the vehicle's appearance. Additionally, the system requires that the driver begins the recognition process by driving beside the target position and pushing a button. Furthermore, [8] showed a comparatively low recognition rate (i.e., 70%). Experimental results showed that the system seen in [8] is affected by reflected sunlight, markings indicating a site for light vehicles, and markings indicating a site for handicapped persons. In comparison, the proposed method can eliminate the influence of such notice markings on the ground surface by reducing the search area and the initial orientation based on the driver's input.

Strong light reflected on a wet ground surface, which is the major cause of recognition interference, is expected to be eliminated by using a polarizing filter [20]. Although we could not quantitatively evaluate the effect as a camera incorporating the filter was unavailable, we could estimate the effect by comparing two images of one scene captured with and without a polarizing filter, as shown in Fig. 20. It is observed that the border of the parking slot markings, which is unseen with strong reflected light as in Fig. 20(a), becomes clearer in Fig. 20(b). Furthermore, as the video gain that was reduced to compensate for strong light in Fig. 20(a) is set to a larger value in Fig. 20(b), the image contrast can be increased.

VI. Conclusion

This paper has proposed a parking slot marking recognition method based on a driver's input for parking-assist systems equipped with a touchscreen. In particular, because the driver can establish the target position by pointing out each side of the entrance of the target parking slot irrespective of the parking slot marking type, the proposed method is expected to be a uniform user interface of driver input-initiated parking slot marking recognition. The system automatically recognizes the parking slot marking type by applying a neural-network-based junction pattern classifier to the area around the driver's input and precisely recognizes the location and orientation of the junction pattern using DT and template matching. The junction pattern localization enables the driver to designate the target position easily and precisely, even in a driving seat, where the exact location could not be clicked.

The contributions of this paper are as follows: 1) This paper has shown that driver input-initiated parking slot marking recognition, or semiautomatic recognition of parking slot markings, can be an efficient parking position-designation method. 2) This paper has proposed a uniform user interface for target position designation, irrespective of parking slot marking type. Furthermore, as the method a driver uses to indicate the junction pattern on each side of the entrance of the target parking slot provides strong constraints upon junction pattern location and orientation, it can significantly reduce the searching range and is intrinsically robust to false classification of the junction pattern. 3) This paper has shown that strong light reflected on a wet ground surface is a major hindrance to parking slot marking recognition and could be reduced by using a polarizing filter. Therefore, this paper recommends that companies developing and producing cameras for parking applications recognize this need and develop methods to embed a polarizing filter into camera modules.

Promising future works are as follows: 1) improvement of neural-network-based junction pattern classification such as input data dimension reduction and adoption of more efficient neural-network architecture, 2) extension of available parking slot marking types, and 3) adaptive binarization that automatically finds the best suitable clustering parameter k by evaluating the performance of binarization with a certain k value.

References

[1] H. G. Jung, Y. H. Cho, P. J. Yoon, and J. Kim, "Scanning laser radar-based target position designation for parking aid system," *IEEE Trans. Intell. Transp. Syst.*, vol. 9, no. 3, pp. 406–424, Sep. 2008.

[2] J. Xu, G. Chen, and M. Xie, "Vision-guided automatic parking for smart car," in *Proc. IEEE Intell. Veh. Symp.*, Oct. 3–5, 2000, pp. 725–730.

[3] H. G. Jung, D. S. Kim, P. J. Yoon, and J. H. Kim, "3D vision system for the recognition of free parking site location," *Int. J. Autom. Technol.*, vol. 7, no. 3, pp. 361–367, May 2006.

[4] H. G. Jung, D. S. Kim, P. J. Yoon, and J. Kim, "Parking slot markings recognition for automatic parking assist system," in *Proc. IEEE Intell. Veh. Symp.*, Tokyo, Japan, Jun. 13–15, 2006, pp. 106–113.

[5] Y. Tanaka, M. Saiki, M. Katoh, and T. Endo, "Development of image recognition for a parking assist system," in *Proc. 13th World Congr. Intell. Transp. Syst. Services*, Oct. 8–12, 2006, pp. 1–7.

[6] H. G. Jung, C. G. Choi, P. J. Yoon, and J. Kim, "Novel user interface for semi-automatic parking assistance system," in *Proc. 31st FISITA World Autom. Congr.*, Oct. 22–27, 2006, pp. 1–10.

[7] H. G. Jung, D. S. Kim, P. J. Yoon, and J. Kim, *Structure Analysis Based Parking Slot Marking Recognition for Semi-Automatic Parking System*, vol. 4109, *Lecture Note in Computer Science*. Berlin, Germany: Springer-Verlag, Aug. 2006, pp. 384–393.

[8] H. Kamiyama, "Parking space detection using side-camera image," in *Proc. 15th World Congr. Intell. Transp. Syst.*, Nov. 16–20, 2008, pp. 1–8.

[9] H. G. Jung, D. S. Kim, P. J. Yoon, and J. Kim, "Two-touch type parking slot marking recognition for target parking position designation," in *Proc. IEEE Intell. Veh. Symp.*, Jun. 4–6, 2008, pp. 1161–1166.

[10] H. G. Jung, Y. H. Lee, P. J. Yoon, and J. Kim, "Radial distortion refinement by inverse mapping-based extrapolation," in *Proc. 18th Int. Conf. Pattern Recog.*, Hong Kong, Aug. 20–24, 2006, pp. 675–678.

[11] P. H. Batavia, D. A. Pomerleau, and C. E. Thorpe, "Overtaking vehicle detection using implicit optical flow," Carnegie Mellon Univ., Pittsburgh, PA, Tech. Rep. Robotics Inst. CMU-RI-TR-97-28, Mar. 4, 1998.

[12] H. Zhang, J. E. Fritts, and S. A. Goldman, "Image segmentation evaluation: A survey of unsupervised methods," *Comput. Vis. Image Underst.*, vol. 110, no. 2, pp. 260–280, May 2008.

[13] *Image Processing Toolbox 6: User's Guide*, Mathworks, Inc., Natick, MA, Oct. 2008, p. 47.

[14] D. M. Gavrila, "Multi-feature hierarchical template matching using distance transforms," in *Proc. IEEE Int. Conf. Pattern Recog.*, Brisbane, Australia, 1998, pp. 439–444.

[15] A. Fong, Skeleton Intersection Detection. Updated on Dec. 18, 2003, accessed on Jan. 14, 2009. [Online]. Available: http://www.mathworks.com/matlabcentral/fileexchange/4254

[16] A. Fong, Skeleton Endpoints. Updated on Dec. 16, 2003, accessed on Jan. 14, 2009. [Online]. Available: http://www.mathworks.com/matlabcentral/fileexchange/4251

[17] H. Demuth, M. Beale, and M. Hagan, *Neural Network Toolbox 5: User's Guide*. Natick, MA: MathWorks, Inc., 2007.

[18] M. F. Moller, "A scaled conjugate gradient algorithm for fast supervised learning," *Neural Netw.*, vol. 6, no. 4, pp. 525–533, 1993.

[19] *Genetic Algorithm and Direct Search Toolbox 2: User's Guide*, Mathworks, Inc., Natick, MA, 2007.

[20] M. Yamada, K. Ueda, I. Horiba, S. Yamamoto, and S. Tsugawa, "Detection of wet-road conditions from images captured by a vehicle-mounted camera," *J. Robot. Mechatron.*, vol. 17, no. 3, pp. 269–276, Jun. 2005.

Ho Gi Jung (M'05) received the B.E., M.E., and Ph.D. degrees from Yonsei University, Seoul, Korea, in 1995, 1997, and 2008, respectively, all in electronic engineering.

From 1997 to April 2009, he was with the Global R&D H.Q., MANDO Corporation, Yongin, Korea. He developed environment-recognition algorithms for lane-departure warning systems and adaptive cruise control from 1997 to 2000. He developed an electronic control unit and embedded software for an electro-hydraulic braking system from 2000 to 2004. Since 2003, he has developed environment-recognition algorithms for intelligent parking-assist systems, collision warning and avoidance, and active pedestrian protection systems. Since May 2009, he has been a Senior Research Engineer with Yonsei University. His interests are automotive vision, driver-assistant systems, active safety vehicles, and intelligent surveillance.

Dr. Jung is a member of the International Society of Automotive Engineering, The International Society for Optical Engineers, which is an international society advancing an interdisciplinary approach to the science and application of light, the Institute of Electronics Engineers of Korea, and the Korean Society of Automotive Engineering.

Yun Hee Lee (M'09) received the B.S. and M.S. degrees from Sogang University, Seoul, Korea, in 2003 and 2005, respectively, both in electronic engineering.

Since 2005, he has been with the Global R&G H.Q., MANDO Corporation, Yongin, Korea, where he has been developing environment-recognition algorithms for collision warning and avoidance systems, lane-keeping assistance systems, and active pedestrian protection systems. His research focuses on driver-assistant systems and automotive vision.

Jaihie Kim (M'84) received the B.S. degree in electronic engineering from Yonsei University, Seoul, Korea, in 1979 and the M.S. degree in data structures and the Ph.D. degree in artificial intelligence from Case Western Reserve University, Cleveland, OH, in 1982 and 1984, respectively.

Since 1984, he has been a Professor with the School of Electrical and Electronic Engineering, Yonsei University. He is currently the Director of the Biometric Engineering Research Center in Korea. His research areas include biometrics, computer vision, and pattern recognition.

Prof. Kim is currently the Chairman of the Korean Biometric Association.